

The Neonicotinoid Electronegative Pharmacophore Plays the Crucial Role in the High Affinity and Selectivity for the *Drosophila* Nicotinic Receptor: An Anomaly for the Nicotinoid Cation– π Interaction Model[†]

Motohiro Tomizawa,^{‡,§} Nanjing Zhang,^{‡,§} Kathleen A. Durkin,^{||} Marilyn M. Olmstead,[⊥] and John E. Casida^{*,‡}

Environmental Chemistry and Toxicology Laboratory, Department of Environmental Science, Policy and Management, and Molecular Graphics Facility, College of Chemistry, University of California, Berkeley, California 94720, and Small Molecule X-ray Crystallography Laboratory, Department of Chemistry, University of California, Davis, California 95616

Received January 10, 2003; Revised Manuscript Received May 5, 2003

ABSTRACT: Cation– π interaction, a prominent feature in agonist recognition by neurotransmitter-gated ion channels, does not apply to the anomalous action of neonicotinoids at the insect nicotinic acetylcholine receptor (nAChR). Insect-selective neonicotinoids have an electronegative pharmacophore (tip) in place of the ammonium or iminium cation of the vertebrate-selective nicotinoids, suggesting topological divergence of the agonist-binding sites in insect and vertebrate nAChRs. This study defines the molecular and electronic basis for the potent and selective interaction of the neonicotinoid electronegative pharmacophore with a unique subsite of the *Drosophila* but not of the vertebrate $\alpha 4\beta 2$ nAChR. Target site potency and selectivity are retained when the usual neonicotinoid *N*-nitroimine (=NNO₂) electronegative tip is replaced with *N*-nitrosoimine (=NNO) or *N*-(trifluoroacetyl)imine (=NCOCF₃) in combination with an imidazolidine, imidazoline, thiazolidine, or thiazoline heterocycle. X-ray crystallography establishes coplanarity between the heterocyclic and imine planes, including the electronegative substituent in the *trans* configuration. The functional tip is the coplanar oxygen atom of the *N*-nitrosoimine or the equivalent oxygen of the *N*-nitroimine. Quantum mechanics in the gas and aqueous phases fully support the conserved coplanarity and projection of the strongly electronegative tip. Further, a bicyclic analogue with a nitro tip in the *cis* configuration but retaining coplanarity has a high potency, whereas the *N*-trifluoromethanesulfonylimine (=NSO₂CF₃) moiety lacking coplanarity confers very low activity. The coplanar system between the electronegative tip and guanidine–amidine moiety extends the conjugation and facilitates negative charge (δ^-) flow toward the tip, thereby enhancing interaction with the proposed cationic subsite such as lysine or arginine in the *Drosophila* nAChR.

Drosophila nicotinic acetylcholine receptors (nAChRs)¹ mediate rapid excitatory neurotransmission and are largely expressed in synaptic neuropil regions of the central nervous system (1). They consist of heteromeric complexes made up of multiple subunits, i.e., four α -type (ALS/D α 1–D α 4) and three β -type (ARD, SBD, and D β 3) with additional candidate subunit genes predicted from genome analyses. However, the functional architecture and diversity of native *Drosophila*

nAChRs are poorly understood compared with those of vertebrate nAChRs (2–6).

Neonicotinoids are one of the most important classes of insecticides, and they are very effective probes for structural investigations of insect nAChRs. They act as agonists at nanomolar levels (4). A neonicotinoid affinity chromatography matrix has been used to isolate the native *Drosophila* nAChR (7). D α 2 is the principal neonicotinoid-binding subunit identified by immunoblotting with a specific antibody (8) and photoaffinity labeling with neonicotinoid radioprobes (9, 10).

Cation– π interaction is a prominent feature in the recognition of agonists by the vertebrate nAChR (11, 12). However, this model does not apply to the anomalous action of neonicotinoids at the insect nAChR. Neonicotinoids have excellent selectivity for insect versus mammalian nAChRs, thereby contributing to the toxicity to insects and safety for mammals. The unique aspect of the neonicotinoid structure is an electron-withdrawing *N*-nitroimine (=NNO₂), *N*-cyanoimine (=NCN), or nitromethylene (=CHNO₂) substituent (Figure 1). In contrast, the nicotinoids, including nicotine, epibatidine, and the *N*-unsubstituted imine (desnitro or descyano) analogues of neonicotinoids (cationic compounds)

[†] This work was supported by NIH Grant R01 ES08424.

^{*} To whom correspondence should be addressed: Environmental Chemistry and Toxicology Laboratory, 114 Wellman Hall, Department of Environmental Science, Policy and Management, University of California, Berkeley, CA 94720-3112. Phone: (510) 642-5424. Fax: (510) 642-6497. E-mail: ectl@nature.berkeley.edu.

[‡] Environmental Chemistry and Toxicology Laboratory, Department of Environmental Science, Policy and Management, University of California, Berkeley.

[§] These authors contributed equally to this study.

^{||} Molecular Graphics Facility, College of Chemistry, University of California, Berkeley.

[⊥] University of California, Davis.

¹ Abbreviations: ACh, acetylcholine; $\alpha 4\beta 2$, major nAChR subtype in vertebrate brain; DFT, density-function theory; ESP, electrostatic potential; IC₅₀, molar concentration of the test compound required for 50% inhibition of specific radioligand binding; IMI or [³H]IMI, imidacloprid or its tritiated form; nAChR, nicotinic ACh receptor.

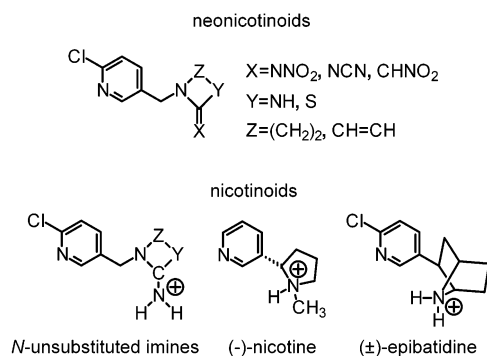


FIGURE 1: Structures of neonicotinoids (X is a nitroimine, cyanoimine, or nitromethylene substituent) selective for the *Drosophila* nAChR and nicotinoids [N-unsubstituted imines, (-)-nicotine, and (±)-epibatidine] selective for the vertebrate nAChR. The neonicotinoids are not protonated, whereas the nicotinoids have a basic nitrogen atom which is protonated at physiological pH.

(Figure 1), selectively interact as nicotinic agonists with the mammalian nAChR subtypes and are selectively toxic to mammals (13–15). This apparent reversal of structure–activity relationships between insects and mammals is attributed to the nonprotonatable property of the neonicotinoids and the cationic nature of the secondary or tertiary amine (ammonium ion) and the N-unsubstituted imine (iminium ion) moieties of nicotinoids under physiological conditions.

This study defines the molecular and electronic basis for the potent and selective interaction of the neonicotinoid electronegative (δ^-) pharmacophore (tip) with a unique cationic subsite of the *Drosophila* nAChR. Eleven ligands are employed as structural probes: N-[(6-chloropyridin-3-yl)methyl]imidazolidines, -imidazolines, -thiazolidines, or -thiazolines with an N-nitroimine ($=\text{NNO}_2$), N-nitrosoimine ($=\text{NNO}$), N-(trifluoroacetyl)imine ($=\text{NCOCF}_3$), or N-trifluoromethanesulfonylimine ($=\text{NSO}_2\text{CF}_3$) substituent (Table 1). Target site potency and selectivity are evaluated for *Drosophila* and vertebrate $\alpha 4\beta 2$ nAChRs. The biological findings are then related to three molecular features of neonicotinoids: conformations and *trans* and *cis* configurations based on X-ray crystallography, electrostatic potential (ESP) mapping on the molecular surface, and energy assessments determined by high-level *ab initio* quantum mechanics. We conclude that the excellent selectivity of neonicotinoids for the insect nAChR can be attributed to an electronegative tip–cationic subsite interaction, the opposite of the nicotinic cation– π interaction model for the vertebrate receptor.

EXPERIMENTAL PROCEDURES

Synthesis. Imidacloprid (IMI, **1a**), 1-(6-chloropyridin-3-ylmethyl)-2-nitroiminoimidazoline (**2a**), and 3-(6-chloropyridin-3-ylmethyl)-2-nitroiminothiazoline (**4a**) were obtained or prepared according to the method of Zhang et al. (16). 1-(6-Chloropyridin-3-ylmethyl)-2-nitrosoiminoimidazoline (**1b**) was synthesized by catalytic reduction of **1a** (17), and the X-ray structure is given in Figure 2. The compounds below were also synthesized specifically for this study and characterized by FAB-HRMS and NMR spectroscopy for solutions in chloroform-*d*.

1-(6-Chloropyridin-3-ylmethyl)-2-nitrosoiminoimidazoline (**2b**). A solution of compound **2c** (prepared as described below) (100 mg, 0.33 mmol) in anhydrous ammonia in

Table 1: Structure–Activity Relationships of Neonicotinoids with N-Nitroimine, N-Nitrosoimine, N-(Trifluoroacetyl)imine, and N-Trifluoromethanesulfonylimine Moieties

neonicotinoid (substituent)	toxicity to housefly ^a mortality (%) (at 0.1 $\mu\text{g/g}$)	receptor potency IC_{50} [nM \pm SD ($n = 3$)] ^b	
		<i>Drosophila</i>	vertebrate $\alpha 4\beta 2$ subtype
imidazolidines (1)			
1a (NNO_2)	74	4.6 ± 0.5	2600 ± 90
1b (NNO)	58	51 ± 5.0	850 ± 26
imidazolines (2)			
2a (NNO_2)	70	1.7 ± 0.7	1700 ± 330
2b (NNO)	50	70 ± 6.2	3500 ± 550
2c (NCOCF_3)	31	7.7 ± 0.7	NT ^c
thiazolidines (3)			
3a (NNO_2)	72	5.7 ± 1.0	1800 ± 160
3b (NNO)	50	4.7 ± 1.3	230 ± 7
thiazolines (4)			
4a (NNO_2)	70	0.70 ± 0.08	620 ± 40
4b (NNO)	52	8.6 ± 0.2	91 ± 11
4c (NCOCF_3)	28	3.1 ± 1.0	NT ^c
4d (NSO_2CF_3)	0	1600 ± 400	NT ^c

^a Pretreated topically with 100 μg of *O*-propyl *O*-(2-propynyl)phenylphosphonate per gram as a P450 inhibitor before intrathoracic administration of the test compound. **4d** was injected at a dose of 5 $\mu\text{g/g}$. All compounds were compared in the same experiment with 50 flies per group and relationships confirmed in a second experiment. ^b Assayed with 3 nM [^3H]IMI and 10 nM [^3H]nicotine binding to the *Drosophila* and $\alpha 4\beta 2$ nAChRs, respectively. ^c Not tested. The corresponding N-unsubstituted imines (possible trace impurities and hydrolysis products) have IC_{50} values of 1–8 nM at the $\alpha 4\beta 2$ receptor but have negligible potency at the *Drosophila* receptor (14).

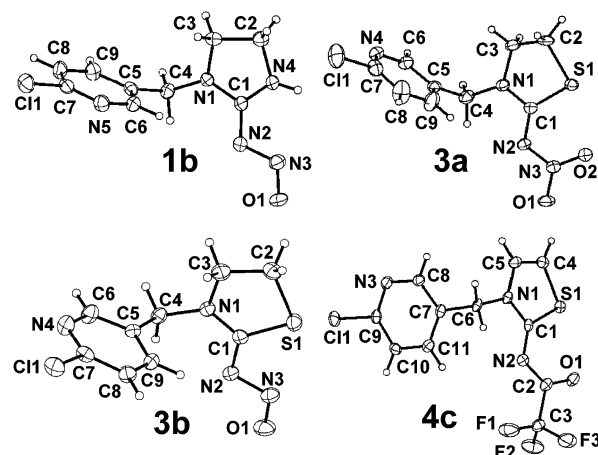


FIGURE 2: X-ray crystallographic structures of neonicotinoids shown as Oak Ridge thermal ellipsoid plots. Although images are not shown, both **1b** and **3b** have two independent molecules in the asymmetric unit.

methanol (2.0 M, 5.0 mL) was stirred at room temperature for 48 h. After evaporation, the residue was purified by preparative silica gel TLC with methylene chloride and methanol (10:1) to give a solid (48 mg, 71%). Into a solution of this material (40 mg, 0.19 mmol) in tetrahydrofuran (2.0 mL) was added isoamyl nitrite (25 μL) at 0 $^{\circ}\text{C}$. The solution was then stirred at room temperature overnight and evapo-

rated, and the residue was purified by silica gel column chromatography with methylene chloride and methanol (10:1) to give **2b** (20 mg, 44%): ^1H NMR δ 8.28 (d, 1H, J = 2.0 Hz), 7.56 (s, 1H), 7.38 (dd, 1H, J = 2.6, 8.2 Hz), 7.32 (d, 1H, J = 8.2 Hz), 7.11 (s, 1H), 6.88 (s, 1H), 5.14 (s, 2H); ^{13}C NMR δ 151.7, 148.4, 137.6, 137.2, 130.8, 130.5, 124.7, 118.9, 47.5.

1-(6-Chloropyridin-3-ylmethyl)-2-trifluoroacetylaminimidazole (**2c**), 3-(6-Chloropyridin-3-ylmethyl)-2-nitroiminothiazolidine (**3a**), 3-(6-Chloropyridin-3-ylmethyl)-2-trifluoroacetylaminothiazoline (**4c**), and 3-(6-Chloropyridin-3-ylmethyl)-2-trifluoromethanesulfonylaminothiazoline (**4d**). The four starting materials were 2-trifluoroacetylaminimidazole (**18**), 2-nitroamino-2-thiazoline (**19**), 2-trifluoroacetylaminothiazole [prepared from 2-aminothiazole by a general procedure (**18**)], and 2-trifluoromethanesulfonylaminothiazole (**20**). They were allowed to react individually (1.0 mmol) with equimolar 6-chloro-3-chloromethylpyridine in the presence of K_2CO_3 (276 mg) in dimethylformamide (5.0 mL) at 55 °C overnight. The solvent was then removed under vacuum and the residue subjected to silica gel chromatography with methylene chloride and methanol (10:1) to give **2c**, **3a**, **4c**, and **4d** as solids (**16**). **2c**: 46% yield; mp 193–195 °C; ^1H NMR δ 12.43 (br s, 1H), 8.44 (br s, 1H), 7.80 (d, 1H, J = 8.2 Hz), 7.52 (d, 1H, J = 8.2 Hz), 7.29 (s, 1H), 6.96 (s, 1H), 5.14 (s, 2H); ^{13}C NMR δ 161.4 (q, J = 33.7 Hz), 149.8, 149.6, 147.3, 139.5, 131.4, 124.2, 117.4 (q, J = 287.5 Hz), 115.7, 113.5, 44.6; FAB-HRMS calcd for $\text{C}_{11}\text{H}_9\text{ClF}_3\text{N}_4\text{O}$ (MH^+) 305.0417, found 305.0412. **3a**: 73% yield; mp 133–134 °C; ^1H NMR δ 8.41 (d, 1H, J = 2.1 Hz), 7.83 (dd, 1H, J = 2.6, 8.2 Hz), 7.55 (d, 1H, J = 8.2 Hz), 4.77 (s, 2H), 3.90 (t, 2H, J = 7.7 Hz), 3.31 (t, 2H, J = 7.7 Hz); ^{13}C NMR δ 174.3, 149.7, 149.4, 139.5, 130.3, 124.3, 51.6, 47.8, 26.9. The X-ray structure is given in Figure 2. **4c**: 73% yield; ^1H NMR δ 8.46 (d, 1H, J = 2.6 Hz), 7.78 (dd, 1H, J = 2.6, 8.2 Hz), 7.36 (d, 1H, J = 8.2 Hz), 7.19 (d, 1H, J = 4.6 Hz), 6.93 (d, 1H, J = 4.6 Hz), 5.43 (s, 2H); ^{13}C NMR δ 161.4 (q, J = 33.7 Hz), 149.8, 149.6, 147.3, 139.5, 131.4, 124.2, 117.4 (q, J = 287.5 Hz), 115.7, 113.5, 44.6. The X-ray structure is given in Figure 2. **4d**: 61% yield; ^1H NMR δ 8.37 (d, 1H, J = 2.1 Hz), 7.67 (dd, 1H, J = 2.1, 8.2 Hz), 7.35 (d, 1H, J = 8.2 Hz), 7.12 (d, 1H, J = 4.6 Hz), 6.79 (d, 1H, J = 4.6 Hz), 5.25 (s, 2H); ^{13}C NMR δ 169.5, 152.0, 149.1, 139.1, 128.8, 126.8, 124.8, 119.8 (q, J = 319.0 Hz), 110.2, 48.9; FAB-HRMS calcd for $\text{C}_{10}\text{H}_8\text{ClF}_3\text{N}_3\text{O}_2\text{S}_2$ (MH^+) 357.9698, found 357.9673.

3-(6-Chloropyridin-3-ylmethyl)-2-nitrosoiminothiazolidine (**3b**). A solution of isoamyl nitrite (0.75 g, 6.4 mmol) in chloroform (2.0 mL) was added to 3-(6-chloropyridin-3-ylmethyl)-2-iminothiazolidine (**21**) (400 mg, 2.1 mmol) in chloroform (10 mL) at 0 °C followed by introduction of a catalytic amount of *p*-toluenesulfonic acid. The solution was stirred overnight at room temperature. Evaporation followed by column chromatography with ethyl acetate and hexane (2:1) provided **3b** as an orange solid (120 mg, 26%): ^1H NMR δ 8.32 (d, 1H, J = 2.6 Hz), 7.64 (dd, 1H, J = 2.6, 8.2 Hz), 7.32 (d, 1H, J = 8.2 Hz), 4.85 (s, 2H), 3.98 (t, 2H, J = 7.7 Hz), 3.39 (t, 2H, J = 7.7 Hz); ^{13}C NMR δ 189.2, 152.1, 149.4, 139.2, 128.8, 125.0, 52.0, 48.3, 26.8; FAB-HRMS calcd for $\text{C}_9\text{H}_{10}\text{ClN}_4\text{O}_2\text{S}$ (MH^+) 257.0264, found 257.0265. The X-ray structure is given in Figure 2.

3-(6-Chloropyridin-3-ylmethyl)-2-nitrosoiminothiazoline (**4b**). To a solution of 3-(6-chloropyridin-3-ylmethyl)-2-iminothiazoline HCl salt (**21**) (260 mg, 1.0 mmol) in water (10 mL) was added sodium nitrite (90 mg, 1.3 mmol) in water (3.0 mL). The solution was adjusted to pH 3–4 with 2 N HCl and stirred for 30 min at room temperature. Methylene chloride (20 mL) was added, and the organic layer was washed with brine and concentrated to dryness to give **4b** as a yellow solid (88 mg, 34%): ^1H NMR δ 8.41 (d, 1H, J = 2.1 Hz), 7.74 (dd, 1H, J = 2.6, 8.2 Hz), 7.42 (d, 1H, J = 4.6 Hz), 7.27 (d, 1H, J = 8.2 Hz), 6.80 (d, 1H, J = 4.6 Hz), 5.53 (s, 2H); ^{13}C NMR δ 152.0, 149.4, 139.1, 129.1, 127.3, 124.7, 110.7, 49.7; FAB-HRMS calcd for $\text{C}_9\text{H}_8\text{ClN}_4\text{O}_2\text{S}$ (MH^+) 255.0107, found 255.0104.

X-ray Crystallography. Compounds **1b**, **3a**, **3b**, and **4c** were allowed to crystallize from ethanol with slow evaporation at room temperature. X-ray analysis was carried out with a Siemens P4 diffractometer equipped with a LT-2 low-temperature apparatus using a Cu rotating anode X-ray source for **1b**, **3a**, and **3b**. Data for **4c** were collected on a Bruker SMART 1000 diffractometer equipped with a Cryo Industries low-temperature apparatus. Crystal data are available at the Cambridge Crystallographic Data Center (CCDC). Copies of the data can be obtained free of charge from CCDC, 12 Union Road, Cambridge CB2 1EZ, U.K. [fax, (+44) 1223-336-033; e-mail, deposit@ccdc.cam.ac.uk].

Quantum Chemistry Calculations. All density-function theory (DFT) calculations were performed using Jaguar 4.1 release 45 (Schrödinger Inc., Portland, OR) on Linux and Silicon Graphics workstations. Single-point calculations were performed on X-ray crystal structures using a self-consistent field calculation of the DFT wave function with a fine grid density. B3LYP/6-311G** (22–24) was chosen for all systems on the basis of results published for nicotine (25). Optimizations were performed at this same level of theory using the default algorithm. When available, optimizations were started from the X-ray crystal structure data. Solution phase results were similarly constructed, starting with gas phase-optimized systems. Specifically, solution phase energies were calculated using a self-consistent reaction field method. Jaguar's Poisson–Boltzmann solver (26, 27) was utilized with all default settings configured for the water model. Density and potential files were prepared using Jaguar's plot functionality. The plot grids used eight points per angstrom in a box whose extents were configured to be at least 3 Å beyond the atomic nuclei on each Cartesian axis. The ESP image was obtained by mapping the potential onto the van der Waals surface with gOpenMol (version 2.1) (28).

Biology. Receptor binding experiments were performed at pH 7.4. The potency of test compounds for the nAChR from *Drosophila melanogaster* heads was determined by displacement of 3 nM [^3H]IMI binding (7). Binding of 10 nM [^3H]nicotine to the vertebrate $\alpha 4\beta 2$ nAChR subtype expressed in mouse fibroblast M10 cells was performed according to the method of Tomizawa and Casida (29). IC_{50} values (molar concentrations of test compounds for 50% inhibition of specific radioligand binding) were calculated by iterative least-squares regression using Sigmaplot (Jandel Scientific Software, San Rafael, CA). The toxicity of test compounds to adult female houseflies (*Musca domestica*) was evaluated by intrathoracic injection following pretreatment with a P450 inhibitor (30, 31).

RESULTS

Structure–Activity Relationships (Table 1). Four neonicotinoid heterocycles with *N*-nitroimine, *N*-nitrosoimine, *N*-(trifluoroacetyl)imine, or *N*-trifluoromethanesulfonylimine substituents were compared for receptor potency and toxicity to *Musca*. In the imidazolidine, imidazoline, and thiazoline series, the nitroso compounds (**1b**, **2b**, and **4b**) exhibited high affinity for the *Drosophila* nAChR with potency loss of only 11–41-fold compared with the corresponding nitroimine analogues (**1a**, **2a**, and **4a**). Interestingly, thiazolidine neonicotinoids with nitro (**3a**) and nitroso (**3b**) substituents displayed the same high affinity for the *Drosophila* receptor. The new imidazoline and thiazoline neonicotinoids with the 2-(trifluoroacetyl)imine group (**2c** and **4c**) had high affinity for the *Drosophila* nAChR, within 2-fold of that of **1a**. However, compound **4d** with a 2-trifluoromethanesulfonylimine substituent was of greatly diminished receptor potency (516-fold less active than **4c** with the 2-trifluoroacetylamine substituent). All of the parent nitroimines were toxic to *Musca* at a dose of 0.1 $\mu\text{g/g}$ with 70–74% mortality. The other compounds were less toxic with mortality at 0.1 $\mu\text{g/g}$ of 50–58% for the nitrosoimines and 28–31% for the (trifluoroacetyl)imines. Trifluoromethanesulfonylimine **4d** was ineffective even at 5 $\mu\text{g/g}$.

Neonicotinoids with nitroimine and nitrosoimine substituents were poorly effective on the vertebrate $\alpha 4\beta 2$ nAChR subtype ($\text{IC}_{50}\text{s} = 230\text{--}3500$ nM) except compound **4b** which was more potent ($\text{IC}_{50} = 91$ nM). (Trifluoroacetyl)imines **2c** and **4c** and trifluoromethanesulfonylimine **4d** were not tested with the $\alpha 4\beta 2$ nAChR because their *N*-unsubstituted imines (possible trace hydrolysis products) in even 1% amounts would interfere with potency evaluation (Table 1).

The neonicotinoids shown in Table 1 are 11–1000-fold more potent at the *Drosophila* nAChR than the vertebrate $\alpha 4\beta 2$ receptor, a relationship that extends to the nitromethylene and cyanoimine analogues with 267–500-fold selectivity (14, 16).

X-ray Crystallography. (a) *General Geometric Features of Neonicotinoid Crystals.* The crystal structures (Figure 2) define the conformational relationships between the pyridine plane and heterocyclic ring/*N*-substituted imine plane as illustrated here by the N1–C4–C5–C6 (in **1b**, **3a**, and **3b**) or N1–C6–C7–C8 torsion angles (in **4c**). The angle between these two planes is dependent on the *N*-substituents. **1a** (32) and **3a** with the nitro group have similar angles of -62.8° and 119.4° (equivalent to -60.6°), respectively. **1b** and **3b** with the nitroso group have similar angles of -139.1° and 139.7° , respectively. **4c** with the trifluoroacetyl group has an angle of -85.4° .

The intermolecular interactions in the solid state involve a competition between three primary acceptor regions: the chlorine of the pyridinyl group, the nitrogen of the pyridinyl group, and an oxygen atom of the $=\text{NNO}_2$, $=\text{NNO}$, or $=\text{NC}(\text{O})\text{CF}_3$ substituent. However, the balance among these acceptors is easily tipped according to crystal packing so the dominant acceptor is not readily evident. The distances of shortest intermolecular hydrogen bonding with **1a**, the *N*-methyl analogue of **1a** (**methyl-1a**) (32), **1b**, **3a**, **3b**, and **4c** are 3.12, 2.89, —, 3.05, 2.94, and — Å, respectively, for the chlorine atom; >2.8 , 2.43, 2.53, 2.49, 2.49, and 2.76 Å, respectively, for the pyridinyl nitrogen atom; and 2.20, 2.40,

2.48, 2.48, 2.66, and 2.96 Å, respectively, for the oxygen atom. None of these correspond to strong and directional influences in the crystal structures. This is not surprising since in **1a** and **1b** there are intermolecular donor hydrogen atoms from imidazolidine N–H groups, but in all other cases, they are C–H groups. Of the C–H hydrogens, the most acidic one appears to be that next to the pyridinyl chlorine, as it is involved in intermolecular contacts in **1a**, **1b**, **3b**, and **4c**.

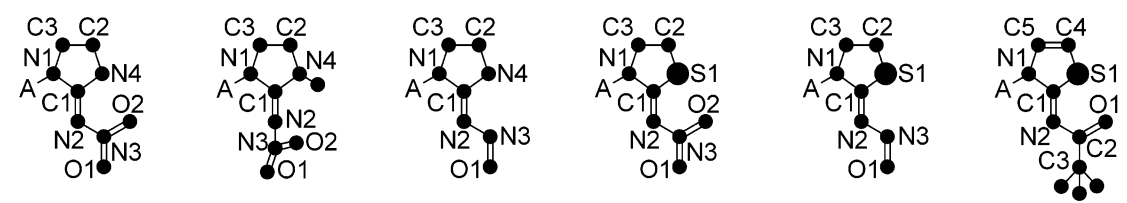
(b) *Orientation and Configuration of the Electron-Withdrawing Tip (Figure 2).* The *N*-nitroimine, *N*-nitrosoimine, or *N*-(trifluoroacetyl)imine substituent in each compound (**1b**, **3a**, **3b**, and **4c**) has the *trans* configuration (*E* in imidazolidine and *Z* in thiazolidine or thiazoline) relative to the chloropyridinylmethyl moiety. The nitroso oxygen atom (O1) in **1b** and **3b** was *anti* to the five-membered ring and horizontally extended from the imine plane. The trifluoromethyl tip of the *N*-(trifluoroacetyl)imine substituent in **4c** was also *anti* to the heterocycle with a horizontal projection.

(c) *Coplanarity between Heterocyclic and N-Substituted Imine Moieties.* One of the common molecular features observed here in **1b**, **3a**, **3b**, and **4c**, as with **1a** and other imidazolidine neonicotinoids (32), was the coplanarity between the heterocyclic ring and the guanidine or amidine moiety with the electron-withdrawing tip, compared as torsion angles and average deviations from least-squares planes (Table 2). The coplanarity between the guanidine or amidine moiety and the electronegative tip is clear from the corresponding torsion angles, all close to 0° or 180° , the N1–C1–N2–N3 angle in **1b**, **3a**, and **3b** and the N1–C1–N2–C2 angle in **4c** as with those for the N1–C1–N2–N3 angle in **1a** (Table 2). In addition, planarity for the five-membered ring was observed in compounds **1b** and **4c** as well as **1a** as indicated by their torsion angles being close to 0° or 180° shown in the third and fourth rows of Table 2. However, the five-membered ring was distorted in compounds **3a** (11.0° for the N1–C1–S1–C2 torsion angle and 26.6° for the C2–C3–N1–C1 torsion angle) and **3b** (8.8° for the C2–C3–N1–C1 torsion angle). In contrast, in **methyl-1a** the N1–C1–N2–N3 torsion angle was twisted by 67.2° and the C2–C3–N1–C1 torsion angle of the imidazolidine plane was also distorted (16.9°) (32). Average deviations from least-squares planes are 0.026–0.030 for **1a**, **1b**, **3b**, and **4c**, confirming the overall coplanarity between the heterocyclic and *N*-substituted imine moieties, and 0.100 (slight distortion) for **3a**. However, major distortion is observed for **methyl-1a** with a value of 0.330 (Table 2).

ESP Surface. The ESP was mapped onto the van der Waals surface of five neonicotinoids (**1a**, **1b**, **3a**, **3b**, and **4c**) and of two corresponding *N*-unsubstituted imines of **1a** and **3a** (protonated at physiological pH). For the neonicotinoids, there is in each case a prominent negative ESP region (illustrated as reddish-orange in Figure 3a) with localization at exactly the same position of the electron-withdrawing group. A significant positive nature is not observed in any case for the N1 atom, while marginally positive ESP is evident for all the atoms of the heterocyclic ring moiety. These molecular shapes are optimized from and consistent with their crystal structures. In marked contrast to the neonicotinoids (Figure 3a), a fully positive cationic character is observed for the protonated *N*-unsubstituted imines (Figure 3b).

Configuration of trans- and cis-1a and Conformation of Bicyclic and N-Trifluoromethanesulfonylimine Analogues. In

Table 2: Coplanarity of Heterocyclic and N-Substituted Imine Moieties of Neonicotinoids Based on X-ray Crystallography^a

					
1a	methyl-1a	1b	3a	3b	4c
comparison by atom sequences and torsion angles (degree) ^a					
C1-N2-N3-O1: 179.5	C1-N2-N3-O1: -171.3	C1-N2-N3-O1: 180.0	C1-N2-N3-O1: 175.1	C1-N2-N3-O1: -177.3	C1-N2-C2-O1: 0.0 ^b
N1-C1-N2-N3: 176.4	N1-C1-N2-N3: 67.2	N1-C1-N2-N3: -174.9	N1-C1-N2-N3: 178.1	N1-C1-N2-N3: 177.7	N1-C1-N2-C2: -177.0
N1-C1-N4-C2: -0.6	N1-C1-N4-C2: 2.7	N1-C1-N4-C2: -2.8	N1-C1-S1-C2: 11.0	N1-C1-S1-C2: -2.8	N1-C1-S1-C4: -1.3
C2-C3-N1-C1: 6.4	C2-C3-N1-C1: -16.9	C2-C3-N1-C1: -2.2	C2-C3-N1-C1: -26.6	C2-C3-N1-C1: 8.8	C4-C5-N1-C1: -1.0
comparison by average deviation from least-squares plane (Å)					
0.030	0.330 ^c	0.026 ^d	0.100	0.030 ^d	0.030

^a A planar moiety gives a torsion angle of 0° or 180°, and divergence from planarity is the difference in the absolute value from 0° or 180°. ^b The C1-N2-C2-C3 torsion angle is -178.8°. ^c The corresponding value without the nitro group is 0.076 Å. ^d A second independent molecule in the asymmetric unit gave a values of 0.041 Å for **1b** and 0.043 Å for **3b**. ^e A in the above structures refers to the 6-chloropyridin-3-ylmethyl moiety (see Table 1). Data for **1a** and **methyl-1a** are based on Kagabu and Matsuno (32).

the gas phase, the *trans E*-isomer of **1a** was more stable than the *cis Z*-isomer (Figure 4) with an energy difference of 9.9 kcal/mol (which corresponds to 0.000005% of the *cis Z*-isomer at the standard temperature). Optimized *trans*-(*E*)-**1a** had a geometry in the gas phase very close to that in the crystal state (32). In addition, the optimized *trans* and *cis* geometries in the gas phase were very similar to those in the aqueous phase where *trans*-(*E*)-**1a** was preferred with an energy difference of 6.7 kcal/mol (corresponding to 0.0012% of the *cis Z*-isomer in the equilibrium state). Thus, *cis*-(*Z*)-**1a** is energetically unfavorable and can therefore not be tested. Accordingly, *cis*-(*Z*)-**1a** was evaluated as the gas phase-optimized structure and found to have significant distortion both in the nitroguanidine plane (C1-N2-N3-O1 and N1-C1-N2-N3 angles distorted by 25.5° and 28.2°) and in the imidazolidine ring (N1-C1-N4-C2 and C2-C3-N1-C1 angles distorted by 16.0° and 17.3°, respectively) (Table 3).

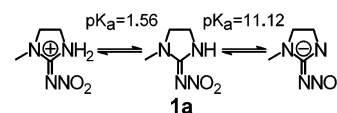
A bicyclic neonicotinoid analogue, 6-methyl-1-[(6-chloro-3-pyridinyl)methyl]-1,2,3,5,6,7-hexahydro-8-nitroimidazo[1,2-*c*]pyrimidine (compound **5**), was of particular interest because the nitro group is *cis* to the chloropyridinylmethyl moiety yet has very high potency (33). In the gas phase-optimized structure, compound **5** was almost flat or slightly distorted (only 4.7–12.2°) in the nitroethene plane (C1-C2-N2-O1 and N1-C1-C2-N2), while torsion angles of the imidazolidine ring (N1-C1-N3-C3 and C3-C4-N1-C1) were distorted 11.6–17.8°, comparable to those in *cis*-(*Z*)-**1a** (Table 3).

The conformation was also examined for the new low-potency (Table 1) *N*-trifluoromethanesulfonylimine derivative

(**4d**) (Table 3). As with the other compounds, the amidine moiety was coplanar with the thiazoline ring as indicated by their torsion angles of 9.6° and 1.7° (N1-C1-N2-S2 and C1-N2-S2-O2, respectively). The thiazoline ring itself was not distorted (torsion angles of 2.7° and 3.5° for N1-C1-S1-C3 and C3-C4-N1-C1, respectively). In contrast to the other neonicotinoids, O1 or C2 of the trifluoromethanesulfonyl moiety (43.2° and 65.8° for C1-N2-S2-O1 and C1-N2-S2-C2, respectively) is oriented out of the coplanar system of the amidine and thiazoline moieties.

DISCUSSION

The neonicotinoids and nicotinoids have some common structural features but are distinctly different in being nonprotonated and predominantly protonated, respectively, at physiological pH. The nonionic nature of neonicotinoids under physiological conditions is evident from comparison of HPLC retention times under neutral, acidic, and basic conditions (14, 34). Further, the principal neonicotinoid IMI (**1a**) has pK_a values of 1.56 and 11.12 (see the structure of **1a**) (35), indicating that <0.0002% of **1a** is protonated at pH 7.4. This feature of neonicotinoids is an obvious deviation from the cationic ligands selective for vertebrate receptors and therefore an anomaly for the nicotinoid cation- π interaction model (11).



The high potency and excellent selectivity of neonicotinoids for the insect nAChR can be attributed to the dif-

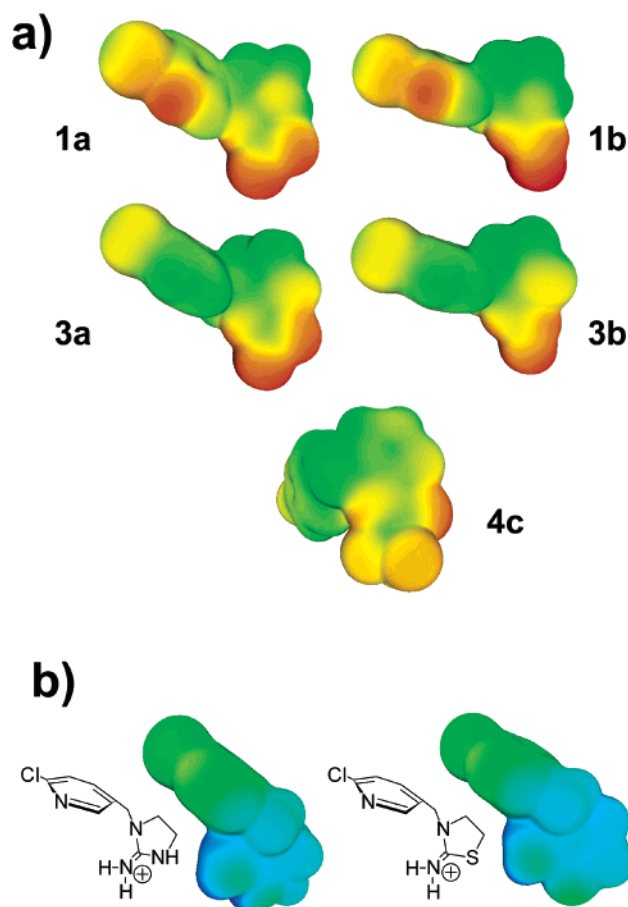


FIGURE 3: Electrostatic potential (ESP) mapping on the molecular surfaces of (a) insect-selective neonicotinoids and (b) vertebrate-selective N-unsubstituted imines (protonated at physiological pH) obtained in the gas phase by high-level *ab initio* calculation with B3LYP/6-311G**. ESP surfaces are shown in red for negative and are graded through orange, yellow, and green to blue for positive with an overall energy range of -60 to 160 kcal/mol. For neonicotinoids (a), optimizations were performed on the basis of crystal structures and the reddish-orange-colored region surrounding the nitro, nitroso or trifluoromethyl group (lower right substituent of each structure) corresponds to the electronegative (δ^-) tip. Although obscured by the angle shown, the N1 atom does not have a significant positive character.

ferential sensitivity of insect versus vertebrate nAChRs, i.e., to topological divergence in their ligand-binding subsites. This hypothesis is addressed here by specifically designing neonicotinoid structural probes featuring variations in the electronegative pharmacophore to delineate biologically suitable conformations and configurations by structure–activity relationship determinations, X-ray crystallography, and high-level computer-based molecular modeling. Two analogues from the literature (**1a** and **methyl-1a**) and a theoretical structure [*cis*-(Z)-**1a**] are used for comparison.

Initial Emphasis on the Role of N1. Nicotinoids are proposed to interact with an aromatic π -electron subsite of the vertebrate nAChR with a major role for the ammonium cation, i.e., cation– π interaction. This hypothesis was modified to fit neonicotinoids, invoking a partially positive charge (δ^+) for the N1 atom conferred by the electron-withdrawing nitro or cyano substituent (36, 37) to propose a binding model also supported by QSAR analysis (38). It was noted that the distance between the van der Waals surfaces of the two nitrogen atoms in nicotine (5.9 Å) is the

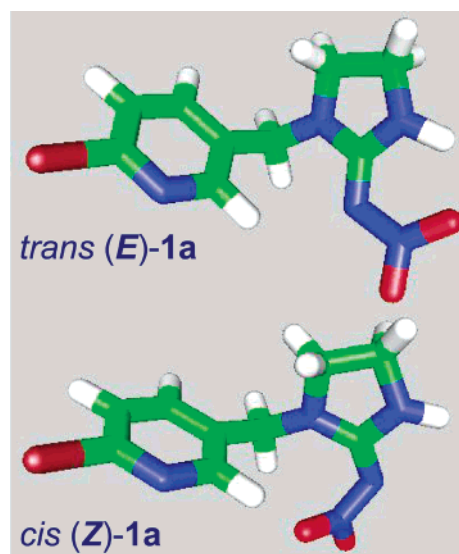


FIGURE 4: Optimized geometries for *trans* (E)- and *cis* (Z)-isomers of **1a** in the gas phase by high-level *ab initio* calculation with B3LYP/6-311G**. Almost the same structures are obtained when optimized in the aqueous phase (images not shown).

same as that between the pyridinyl nitrogen and N1 of the neonicotinoids (5.45 – 6.06 Å), consistent with the ammonium nitrogen and carboxyl oxygen atoms of acetylcholine (ACh) (32). The same relationship was also found in the distance between N1 (or N4) and O1 of **1a** (32). However, the neonicotinoid N1 atom is marginally positive on the basis of ESP, Mulliken atomic charge distribution, and ^{15}N NMR, and this is not correlated to the binding affinity (refs 14 and 39 and this report). Although this weak positive charge on N1 may be slightly improved when the interaction of the nitro oxygen atom with a putative residue of the receptor (via hydrogen-bonding) is included in a PM3 calculation (40), this slightly inducible N1 δ^+ is not comparable to that of the fully positive ammonium nitrogen atom of vertebrate nicotinic agonists and therefore does not explain the outstanding potency and excellent selectivity of **1a** compared with those of nicotine (~ 1000 -fold) at the *Drosophila* receptor (14). Further, neonicotinoid N1 is of sp^2 nature, and the deficient 2p orbital lobes extend vertically with respect to the heterocyclic ring; i.e., interaction of this nitrogen atom with the insect receptor is restricted to this direction only (32). This differs from the sp^3 nature of the ammonium or pyrrolidinyl nitrogen of nicotine. Interestingly, N1 can be replaced with a carbon atom with retention of significant insecticidal activity (41). Thus, N1 of neonicotinoids may only play a complementary role in the binding interaction and/or selectivity. Other molecular aspects were therefore considered in modeling the neonicotinoid agonist-binding site in the *Drosophila* nAChR.

Electronegative Tip. A unique feature of the neonicotinoids is their strongly electronegative tip observed according to the ESP maps at the oxygen (for **1a**, **1b**, **3a**, and **3b**) or trifluoromethyl substituent (for **4c**). Again, there is not sufficient positive charge on N1 to balance the strong electronegative charge of the nitro oxygen area, which is evident in the high-level *ab initio* calculations presented here. Considering the push–pull relationship in this electronic system, the corresponding positive charge instead disperses into the whole heterocycle moiety. The orientation of the

Table 3: Coplanarity of Heterocyclic and N-Substituted Imine-Derived Moieties of Bicyclic Analogue **5**, the *Cis Z*-Isomer of **1a**, and Trifluoromethanesulfonylimine **4d** in the Gas Phase by High-Level *ab Initio* Calculation with B3LYP/6-311G**

5	<i>cis (Z)</i> - 1a	4d
comparison by atom sequences and torsion angles (degree) ^a		
C1-C2-N2-O1: 175.3	C1-N2-N3-O1: 154.5	C1-N2-S2-O2: -1.7
N1-C1-C2-N2: -12.2	N1-C1-N2-N3: -28.2	C1-N2-S2-O1: 136.8
N1-C1-N3-C3: 11.6	N1-C1-N4-C2: -16.0	C1-N2-S2-C2: -114.2
C3-C4-N1-C1: -17.8	C2-C3-N1-C1: 17.3	N1-C1-N2-S2: 170.4
		N1-C1-S1-C3: 3.5
		C3-C2-N1-C1: 2.7

^a A planar moiety gives a torsion angle of 0° or 180°, and divergence from planarity is the difference in the absolute value from 0° or 180°.

electronegative tip might play an important role in activity. The *N*-nitrosoimines lack the nitro O2 yet retain high affinity for the *Drosophila* nAChR, thereby indicating O1 is the minimum electron-rich tip for binding. The electronegative nitroso oxygen (O1) of **1b** or **3b** (and possibly by analogy of **2b** or **4b**) projects horizontally from the imine plane to the outside rather than to the position of O2 in the nitroimines (**1a**, **2a**, **3a**, or **4a**), suggesting that O1 interacts with the putative subsite of the *Drosophila* receptor. By analogy, the horizontal trifluoromethyl extension of the (trifluoroacetyl)-imine moiety corresponds to the O1 atom and would serve as the tip of **4c**.

In marked contrast to the neonicotinoids, the ESP surfaces of N-unsubstituted imines (protonated at physiological pH) with selectivity for the vertebrate nAChRs are strongly positive. As with the cationic ligands nicotine and epibatidine, the two N-unsubstituted imines with imidazolidine and thiazolidine rings are highly active at the vertebrate $\alpha 4\beta 2$ nAChR (affinities of 8 and 4 nM, respectively) but are less active at the *Drosophila* receptor (1500 and 200 nM, respectively) (14).

Coplanarity between Heterocyclic and N-Substituted Imine Planes. Coplanarity between the heterocyclic and imine planes, including an electronegative substituent, is considered to be an essential feature for high affinity at the *Drosophila* receptor. In **1a**, O2 of the nitro group forms a pseudoring via intramolecular bonding with hydrogen on imidazolidine N4 (O2–H distance = 2.1 Å), thereby consolidating the coplanarity (32). *N*-Nitrosoimine **1b** (also expected for **2b**) without the additional O2 maintains the coplanarity and retains the high level of receptor potency. Thiazoline **4c** (and probably imidazoline **2c**) with the trifluoroacetyl-imine tip also conserves the coplanarity between the imine plane and the heterocyclic ring. Imidazoline and thiazoline compounds **2a** and **4a** have enhanced binding affinity compared with their imidazolidine and thiazolidine analogues **1a** and **3a**,

respectively; the double bond may stabilize the planarity of the heterocycle as observed in comparing torsion angles of the thiazolidine and thiazoline rings in **3a** and **4c**. A particularly interesting observation is the equal very high potency of the thiazolidine nitroimine (**3a**) and nitrosoimine (**3b**) even though the heterocyclic ring is flatter in the latter case. Two analogues lack the required coplanarity and have low insect receptor potency. Thus, **methyl-1a** does not have the coplanarity of **1a** (32) and is almost 3000-fold less active at the target site (30). The very low receptor potency of **4d** with the strong electron-withdrawing *N*-trifluoromethanesulfonylimine substituent also can be attributed to the drastically disrupted planarity of O1 and C2, but the steric hindrance of the trifluoromethanesulfonyl group might also be a contributing factor. This strongly supports the hypothesis that O1 (with coplanarity) of the *N*-nitroimine or *N*-nitrosoimine is the functional tip. Therefore, as an explanation for the importance of coplanarity for binding, the orientation of the heterocyclic and imine moieties (with the electronegative group) extends the conjugation (resonance) of the system. This facilitates negative charge (δ^-) flow toward the tip.

Trans/Cis Configuration. The configuration of neonicotinoids may be different in solution from that in the crystal state, prompting us to use quantum chemical optimization for **1a**. The *trans*-(*E*)-**1a** form is predominant in both the gas and aqueous phases (Figure 4). In both phases, the calculated geometry for *trans*-(*E*)-**1a** is very close to that observed by X-ray crystallography. Analogues of **1a** and **3a** with nitromethylene and *N*-cyanoimine (thiacloprid) substituents, respectively, are identified as *trans* isomers (*E* in the former case and *Z* in the latter) on the basis of nuclear Overhauser enhancement NMR spectroscopy experiments in dimethyl sulfoxide-*d*₆ or chloroform-*d* (16, 42). Thiacloprid is in the *trans* (*Z*)-configuration based on the crystal geometry and calculated optimization (DFT) in the

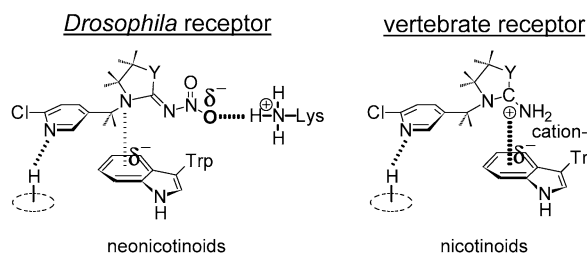


FIGURE 5: Molecular models of binding subsites in the *Drosophila* or vertebrate nAChR for electronegative (δ^-) neonicotinoids or cationic nicotinoids, respectively. The nicotinoid shown represents a desnitro or descyano neonicotinoid. The electronegative oxygen or equivalent tip in the neonicotinoid molecule interacts (perhaps through electrostatic interaction and/or via hydrogen bonding) with the *Drosophila* nAChR subsite consisting of putative cationic amino acid residue(s) such as lysine (or arginine). In contrast, the nitrogen atom of the N-unsubstituted imine serves as a proton acceptor generating a positive charge on the nitrogen and/or carbon atom of the imine moiety ($^+C-NH_2 \leftrightarrow C=^+NH_2$) under physiological conditions (14). This iminium cation, as with the ammonium nitrogen in nicotine and epibatidine, interacts with a specific vertebrate nAChR subsite consisting of aromatic residues (cation- π interaction). Neonicotinoid N1 with an sp^2 nature may undergo complementary interaction with the π -electrons of the aromatic amino acid residue ($p-\pi$ interaction) on the *Drosophila* receptor (32, 36, 37). The nitrogen atom of the pyridinyl ring is also an important factor (4, 14).

gas and water phases with energy differences of 4 and 5 kcal/mol, respectively (42).

The *trans/cis* configuration takes on special interest in comparing *trans*-(*E*)-**1a** with *cis*-(*Z*)-**1a** and the conformationally constrained **5** with the nitro group in the *cis* position. The nitroimine plane of *cis*-(*Z*)-**1a** is greatly distorted (perhaps due to steric crowding), similar to that found for the crystal geometry of **methyl-1a** (32). This suggests that, even though it cannot be tested, *cis*-(*Z*)-**1a** is probably of low activity at the target site as with **methyl-1a**. The bicyclic analogue **5** (with a nitro group in the *cis* position) has almost the same potency as **1a** as an inhibitor of [3H]IMI binding to *Musca* nAChR (33). Interestingly, the degree of distortion in the nitroethene plane in **5** is significantly lower than those observed in the nitroimine plane of *cis*-(*Z*)-**1a** and **methyl-1a**. Thus, this apparent discrepancy may be overcome by the conserved planarity and/or the orientation of the nitro O1 tip in **5**, allowing approach to the subsite. Alternatively, the increased lipophilicity of **5** may be involved. This bicyclic analogue (i.e., Mannich adduct) probably acts directly rather than reverting to the nitromethylene precursor since it is fairly stable at physiological pH, at least during assays (9, 43).

Neonicotinoid-Binding Subsites in *Drosophila* Receptor. The new findings and discussion above focus on three structural features of neonicotinoids that play an essential role in the high affinity and selectivity for the *Drosophila* nAChR, i.e., the noncationic nature, the electronegative tip, and the coplanarity between the electronegative tip and the substituted guanidine-amidine moiety. The electronegative pharmacophore is considered to be crucial in the specific recognition of insect-selective neonicotinoids by a putative unique subsite. The coplanarity makes a conjugated electronic system facilitating negative charge flow toward the tip to consolidate the binding. The putative subsite is proposed to be cationic, possibly lysine or arginine, associating with the electronegative tip perhaps through electrostatic interaction and/or hydrogen bonding (left panel in Figure 5). Lysine and

arginine are prominent (and histidine minor) in the extracellular domain of D α 2 (44) which is the main neonicotinoid-binding subunit (8–10). Although no direct information is available about the location of the relevant cationic residue(s), photoaffinity labeling with a suitable neonicotinoid ligand (16) coupled with computer-assisted docking simulation (45) may help define the orientation of the neonicotinoid electronegative tip in the binding domain. These studies will facilitate understanding the crucial molecular difference between insect and vertebrate receptors conferring neonicotinoid selectivity.

CONCLUSION

Agonist ligands acting at the superfamily of neurotransmitter-gated ion channels (including nicotinic, γ -aminobutyric acid, glycine, and serotonin type 3 receptors) are characteristically cationic in nature. In vertebrate systems, the iminium cation of N-unsubstituted imine analogues of neonicotinoids or ammonium nitrogen of nicotine, epibatidine, or ACh binds to the subsite (14) (right panel in Figure 5) which is surrounded by aromatic residues, including the critical tryptophan of α 1, α 4, and α 7 subunits (and also a snail ACh-binding protein); i.e., the cation makes van der Waals contact with the π -electrons (δ^-) of the aromatic amino acid residues (12, 45–47). As an anomaly, neonicotinoid agonists are noncationic and instead provide an electronegative tip to be recognized by the insect receptor subsite. This topological divergence in *Drosophila* versus vertebrate receptor subsites therefore serves as the basis for the electronegative pharmacophore (e.g., nitro or cyano group) determining the excellent selectivity and potency of neonicotinoids.

ACKNOWLEDGMENT

We received valuable advice and assistance from our laboratory colleagues Hsiao-Lin Chin, David Lee, and Gary Quistad. Quantum mechanics calculations were performed on workstations donated by Dell.

REFERENCES

- Gundelfinger, E. D., and Schultz, R. (2000) Insect nicotinic acetylcholine receptors: genes, structure, physiological and pharmacological properties, in *Handbook of Experimental Pharmacology, Volume 144: Neuronal Nicotinic Receptors* (Clementi, F., Fornasari, D., and Gotti, C., Eds.) pp 497–521, Springer-Verlag, Berlin.
- Littleton, J. T., and Ganetzky, B. (2000) Ion channels and synaptic organization: analysis of the *Drosophila* genome, *Neuron* 26, 35–43.
- Tomizawa, M., and Casida, J. E. (2001) Structure and diversity of insect nicotinic acetylcholine receptors, *Pest Manag. Sci.* 57, 914–922.
- Tomizawa, M., and Casida, J. E. (2003) Selective toxicity of neonicotinoids attributable to specificity of insect and mammalian nicotinic receptors, *Annu. Rev. Entomol.* 48, 339–364.
- Chamaon, K., Smalla, K.-H., Thomas, U., and Gundelfinger, E. D. (2002) Nicotinic acetylcholine receptors of *Drosophila*: three subunits encoded by genomically linked genes can co-assemble into the same receptor complex, *J. Neurochem.* 80, 149–157.
- Lansdell, S. J., and Millar, N. S. (2002) D β 3, an atypical nicotinic acetylcholine receptor subunit from *Drosophila*: molecular cloning, heterologous expression and coassembly, *J. Neurochem.* 80, 1009–1018.
- Tomizawa, M., Latli, B., and Casida, J. E. (1996) Novel neonicotinoid-agarose affinity column for *Drosophila* and *Musca* nicotinic acetylcholine receptors, *J. Neurochem.* 67, 1669–1676.

8. Schulz, R., Bertrand, S., Chamaon, K., Smalla, K.-H., Gundelfinger, E. D., and Bertrand, D. (2000) Neuronal nicotinic acetylcholine receptors from *Drosophila*: two different types of α subunits coassemble within the same receptor complex, *J. Neurochem.* 74, 2537–2546.
9. Tomizawa, M., and Casida, J. E. (1997) [125 I]Azidonicotinoid photoaffinity labeling of insecticide-binding subunit of *Drosophila* nicotinic acetylcholine receptor, *Neurosci. Lett.* 237, 61–64.
10. Tomizawa, M., Wen, Z., Chin, H.-L., Morimoto, H., Kayser, H., and Casida, J. E. (2001) Photoaffinity labeling of insect nicotinic acetylcholine receptors with a novel [3 H]azidoneonicotinoid, *J. Neurochem.* 78, 1359–1366.
11. Dougherty, D. A. (1996) Cation- π interactions in chemistry and biology: a new view of benzene, Phe, Tyr, and Trp, *Science* 271, 163–168.
12. Zhong, W., Gallivan, J. P., Zhang, Y., Li, L., Lester, H. A., and Dougherty, D. A. (1998) From *ab initio* quantum mechanics to molecular neurobiology: a cation- π binding site in the nicotinic receptor, *Proc. Natl. Acad. Sci. U.S.A.* 95, 12088–12093.
13. Tomizawa, M., and Casida, J. E. (1999) Minor structural changes in nicotinoid insecticides confer differential subtype selectivity for mammalian nicotinic acetylcholine receptors, *Br. J. Pharmacol.* 127, 115–122.
14. Tomizawa, M., Lee, D. L., and Casida, J. E. (2000) Neonicotinoid insecticides: molecular features conferring selectivity for insect versus mammalian nicotinic receptors, *J. Agric. Food Chem.* 48, 6016–6024.
15. Tomizawa, M., Cowan, A., and Casida, J. E. (2001) Analgesic and toxic effects of neonicotinoid insecticides in mice, *Toxicol. Appl. Pharmacol.* 177, 77–83.
16. Zhang, N., Tomizawa, M., and Casida, J. E. (2002) Structural features of azidopyridinyl neonicotinoid probes conferring high affinity and selectivity for mammalian $\alpha 4\beta 2$ and *Drosophila* nicotinic receptors, *J. Med. Chem.* 45, 2832–2840.
17. Novák, L., Hornyánszky, G., Király, I., Rohály, J., Kolonits, P., and Szántay, C. (2001) Preparation of new imidacloprid analogues, *Heterocycles* 55, 45–57.
18. Lee, H. C., Kumar, P., Wiebe, L. I., McDonald, R., Mercer, J. R., Ohkura, K., and Seki, K.-i. (1999) Synthesis of iodoaminoimidazole arabinoside (IAIA): a potential reductive metabolite of the spect imaging agent, iodoazomycin arabinoside (IAZA), *Nucleosides Nucleotides* 18, 1995–2016.
19. Isao, A., and Isao, M. (1993) Preparation of nitroguanidines as agrochemicals, Jpn. Kokai Tokkyo Koho JP 05112521.
20. Trepka, R. D., Harrington, J. K., McConville, J. W., McGurran, K. T., Mendel, A., Pauly, D. R., Robertson, J. E., and Waddington, J. T. (1974) Synthesis and herbicidal activity of fluorinated N-phenylalkanesulfonamides, *J. Agric. Food Chem.* 22, 1111–1119.
21. Latli, B., D'Amour, K., and Casida, J. E. (1999) Novel and potent 6-chloro-3-pyridinyl ligands for the $\alpha 4\beta 2$ neuronal acetylcholine receptor, *J. Med. Chem.* 42, 2227–2234.
22. Becke, A. D. (1988) Density-functional exchange-energy approximation with correct asymptotic-behavior, *Phys. Rev. A* 38, 3098–3100.
23. Lee, C. T., Yang, W. T., and Parr, R. G. (1988) Development of the Colle-Salvetti correlation-energy formula into a functional of the electron-density, *Phys. Rev. B* 37, 785–789.
24. Miehlich, B., Savin, A., Stoll, H., and Preuss, H. (1989) Results obtained with the correlation-energy density functionals of Becke and Lee, Yang and Parr, *Chem. Phys. Lett.* 157, 200–206.
25. Elmore, D. E., and Dougherty, D. A. (2000) A computational study of nicotine conformations in the gas phase and in water, *J. Org. Chem.* 65, 742–747.
26. Tannor, D. J., Marten, B., Murphy, R., Friesner, R. A., Sitkoff, D., Nicholls, A., Ringnalda, M., Goddard, W. A., and Honig, B. (1994) Accurate first principles calculation of molecular charge-distributions and solvation energies from *ab initio* quantum-mechanics and continuum dielectric theory, *J. Am. Chem. Soc.* 116, 11875–11882.
27. Marten, B., Kim, K., Cortis, C., Friesner, R. A., Murphy, R. B., Ringnalda, M. N., Sitkoff, D., and Honig, B. (1996) New model for calculation of solvation free energies: correction of self-consistent reaction field continuum dielectric theory for short-range hydrogen-bonding effects, *J. Phys. Chem.* 100, 11775–11788.
28. Laaksonen, L. (1992) A graphics program for the analysis and display of molecular dynamics trajectories, *J. Mol. Graphics* 10, 33–34.
29. Tomizawa, M., and Casida, J. E. (2000) Imidacloprid, thiacloprid, and their imine derivatives up-regulate the $\alpha 4\beta 2$ nicotinic acetylcholine receptor in M10 cells, *Toxicol. Appl. Pharmacol.* 169, 114–120.
30. Liu, M.-Y., Lanford, J., and Casida, J. E. (1993) Relevance of [3 H]imidacloprid binding site in house fly head acetylcholine receptor to insecticidal activity of 2-nitromethylene- and 2-nitroimino-imidazolidines, *Pestic. Biochem. Physiol.* 46, 200–206.
31. Yamamoto, I., Tomizawa, M., Saito, T., Miyamoto, T., Walcott, E. C., and Sumikawa, K. (1998) Structural factors contributing to insecticidal and selective actions of neonicotinoids, *Arch. Insect Biochem. Physiol.* 37, 24–32.
32. Kagabu, S., and Matsuno, H. (1997) Chloronicotinyl insecticides. 8. Crystal and molecular structures of imidacloprid and analogous compounds, *J. Agric. Food Chem.* 45, 276–281.
33. Latli, B., Tomizawa, M., and Casida, J. E. (1997) Synthesis of a novel [125 I]neonicotinoid photoaffinity probe for the *Drosophila* nicotinic acetylcholine receptor, *Bioconjugate Chem.* 8, 7–14.
34. Kagabu, S., and Medej, S. (1995) Stability comparison of imidacloprid and related compounds under simulated sunlight, hydrolysis conditions, and to oxygen, *Biosci., Biotechnol., Biochem.* 59, 980–985.
35. Chamberlain, K., Evans, A. A., and Bromilow, R. H. (1996) 1-Octanol/water partition coefficient (K_{ow}) and pK_a for ionisable pesticides measured by a pH-metric method, *Pestic. Sci.* 47, 265–271.
36. Tomizawa, M., and Yamamoto, I. (1993) Structure–activity relationships of nicotinoids and imidacloprid analogs, *J. Pestic. Sci.* 18, 91–98.
37. Yamamoto, I., Yabuta, G., Tomizawa, M., Saito, T., Miyamoto, T., and Kagabu, S. (1995) Molecular mechanism for selective toxicity of nicotinoids and neonicotinoids, *J. Pestic. Sci.* 20, 33–40.
38. Okazawa, A., Akamatsu, M., Ohoka, A., Nishiwaki, H., Cho, W.-J., Nakagawa, Y., Nishimura, K., and Ueno, T. (1998) Prediction of the binding mode of imidacloprid and related compounds to house-fly head acetylcholine receptors using three-dimensional QSAR analysis, *Pestic. Sci.* 54, 134–144.
39. Nakayama, A., and Sukekawa, M. (1998) Quantitative correlation between molecular similarity and receptor-binding activity of neonicotinoid insecticides, *Pestic. Sci.* 52, 104–110.
40. Matsuda, K., Buckingham, S. D., Kleier, D., Rauh, J. J., Grauso, M., and Sattelle, D. B. (2001) Neonicotinoids: insecticides acting on insect nicotinic acetylcholine receptors, *Trends Pharmacol. Sci.* 22, 573–580.
41. Boëlle, J., Schneider, R., Gérardin, P., Loubinoux, B., Maienfisch, P., and Rindlisbacher, A. (1998) Synthesis and insecticidal evaluation of imidacloprid analogs, *Pestic. Sci.* 54, 304–307.
42. Jeschke, P., Moriya, K., Lantzsche, R., Seifer, H., Lindner, W., Jelic, K., Göhr, A., Beck, M. E., and Etzel, W. (2001) Thiacloprid (Bay YRC 2894): A new member of the chloronicotinyl insecticide (CNI) family, *Pflanzenschutz-Nachr. Bayer* 54, 147–160.
43. Nauen, R., Ebbinghaus-Kintscher, U., Elbert, A., Jeschke, P., and Tietjen, K. (2001) Acetylcholine receptors as sites for developing neonicotinoid insecticides, in *Biochemical Sites of Insecticide Action and Resistance* (Ishaaya, I., Ed.) pp 77–105, Springer-Verlag, Berlin.
44. Gundelfinger, E. D., and Hess, N. (1992) Nicotinic acetylcholine receptors of the central nervous system of *Drosophila*, *Biochim. Biophys. Acta* 1137, 299–308.
45. Le Novère, N., Grutter, T., and Changeux, J.-P. (2002) Models of the extracellular domain of the nicotinic receptors and of agonist- and Ca^{2+} -binding sites, *Proc. Natl. Acad. Sci. U.S.A.* 99, 3210–3215.
46. Beene, D. L., Brandt, G. S., Zhong, W., Zacharias, N. M., Lester, H. A., and Dougherty, D. A. (2002) Cation- π interactions in ligand recognition by serotonergic (5-HT $_3A$) and nicotinic acetylcholine receptors: the anomalous binding properties of nicotine, *Biochemistry* 41, 10262–10269.
47. Brejc, K., van Dijk, W. J., Klaassen, R. V., Schuurmans, M., van der Oost, J., Smit, A. B., and Sixma, T. K. (2001) Crystal structure of an ACh-binding protein reveals the ligand-binding domain of nicotinic receptors, *Nature* 411, 269–276.